INVERSE PREDICTION OF THE CALPHAD-MODELED PHYSICAL PROPERTIES OF SUPERALLOYS USING EXPLAINABLE ARTIFICIAL INTELLIGENCE AND ARTIFICIAL NEURAL NETWORKS

Yusuf UZUNOĞLU [1*] [iD], Yusuf ALACA [2] [iD]

[1] *Erciyes University, Materials Science and Engineering Department, Kayseri, Türkiye*

[2] *Hitit University, Computer Engineering Department, Çorum, Türkiye*

*** Corresponding Author:** yusufuzunoglu11@gmail.com*

ABSTRACT

The CALPHAD methodology models the physical, mechanical, and thermodynamic properties of materials based on specified alloy compositions using phase equilibrium calculations and thermodynamic databases. With the CALPHAD approach, millions of material-property data can be obtained for each alloy composition over various temperature ranges. However, finding an alloy with the desired properties often requires lengthy trial-and-error processes that involve manually adjusting the composition. In this study, the goal is to inverse this approach using artificial intelligence to predict alloy compositions that yield the desired properties. Accordingly, in the JMatPro software based on the CALPHAD methodology, the physical properties (density, thermal conductivity, linear expansion, Young's modulus, bulk modulus, shear modulus, and Poisson's ratio) of 250 different Ni-Cr-Fe-based superalloys in the temperature range of 540–920 °C were modeled. A dataset with 5000 rows was created from the generated data, of which 80% was used to train the artificial intelligence model, while 20% was reserved for validation and testing. Through analyses using Explainable Artificial Intelligence (XAI) and Artificial Neural Networks (ANN), alloy compositions with the desired physical properties at a given temperature were predicted with a high accuracy rate of 98.03%. In conclusion, beyond obtaining material properties from alloy compositions through the CALPHAD approach, artificial intelligence techniques make it possible to accurately inverse predict alloy compositions that yield specified physical properties at a particular temperature.

Keywords: CALPHAD methodology, Explainable artificial intelligence, Artificial neural networks, Alloy design, Superalloy.

1   INTRODUCTION

The design and development of high-performance alloys, particularly superalloys, require precise control of their physical and mechanical properties at elevated temperatures. Traditional alloy design relies heavily on the CALPHAD (Calculation of Phase Diagrams) methodology, which utilizes phase equilibrium calculations and thermodynamic databases to model material properties based on specific alloy compositions [1]. By inputting alloy composition parameters, researchers can obtain extensive property data across temperature ranges, offering invaluable insights into alloy behavior under various conditions [2]. However, identifying compositions that achieve the target properties often necessitates labor-intensive adjustments and trial-and-error iterations, particularly for superalloys with complex requirements [3].

Artificial intelligence (AI) holds promise in material design because it can make rapid predictions from large datasets and perform inverse predictions of targeted properties [4] [5]. For instance, recent studies have demonstrated that Explainable Artificial Intelligence (XAI) and Artificial Neural Networks (ANNs) can effectively predict material properties and composition relationships, enhancing the efficiency of alloy design [6]. Unlike traditional methods, these AI-driven approaches leverage existing data to predict alloy compositions that satisfy specific mechanical and thermophysical requirements, thus reducing the experimental workload [7].

This study aims to address the limitations of the traditional CALPHAD approach by implementing an inverse prediction model. By using JMatPro software to model the physical properties of Ni-Cr-Fe-based superalloys within a targeted temperature range (540–920 °C), this work leverages AI to predict the alloy compositions necessary to achieve the desired properties. Our method expands on previous work by combining CALPHAD with artificial intelligence to improve prediction accuracy and the interpretability of results [8] [9]. This hybrid approach enables high-accuracy prediction of alloy compositions that exhibit specific physical characteristics, achieving a prediction accuracy of 98.03% in our experiments. Thus, our study provides a novel solution for inverse alloy design that complements existing computational tools in materials science [10].

2   MATERIALS AND METHODS

In this study, the JMatPro software, based on the CALPHAD methodology, was utilized to model the physical properties (density, thermal conductivity, linear expansion coefficient, Young's modulus, bulk modulus, shear modulus, and Poisson's ratio) of Ni-Cr-Fe-based superalloys (Inconel, Incoloy). A dataset of 5000 rows was generated from the obtained data, with 80% allocated to training the artificial intelligence (AI) model and 20% reserved for validation and testing. The AI model was developed using Explainable Artificial Intelligence (XAI) and Artificial Neural Networks (ANNs).

The proposed model (Figure 1) operates on a dataset containing 250 different compositions of Ni, Cr, Fe, Co, Mo, Si, Mn, Ti, Al, Nb, and Cu. The physical properties of these compositions (density, linear expansion, thermal conductivity, Young's modulus, bulk modulus, shear modulus, and Poisson's ratio) were calculated using the CALPHAD method. The obtained data were subjected to a normalization process before being used as input to the model. The normalized data were then fed into an artificial neural network (ANN) model, and the model outputs were analyzed using Explainable Artificial Intelligence (XAI) methods. This analysis process evaluated the effects of physical properties and temperature by classifying them into positive and negative impacts. The accuracy of the model results was validated through comparison with JMatPro software. Consequently, in contrast to the conventional approach of the CALPHAD methodology, which models the physical properties of materials based on their composition, this study successfully performed inverse modeling to determine the compositions corresponding to the desired physical properties.
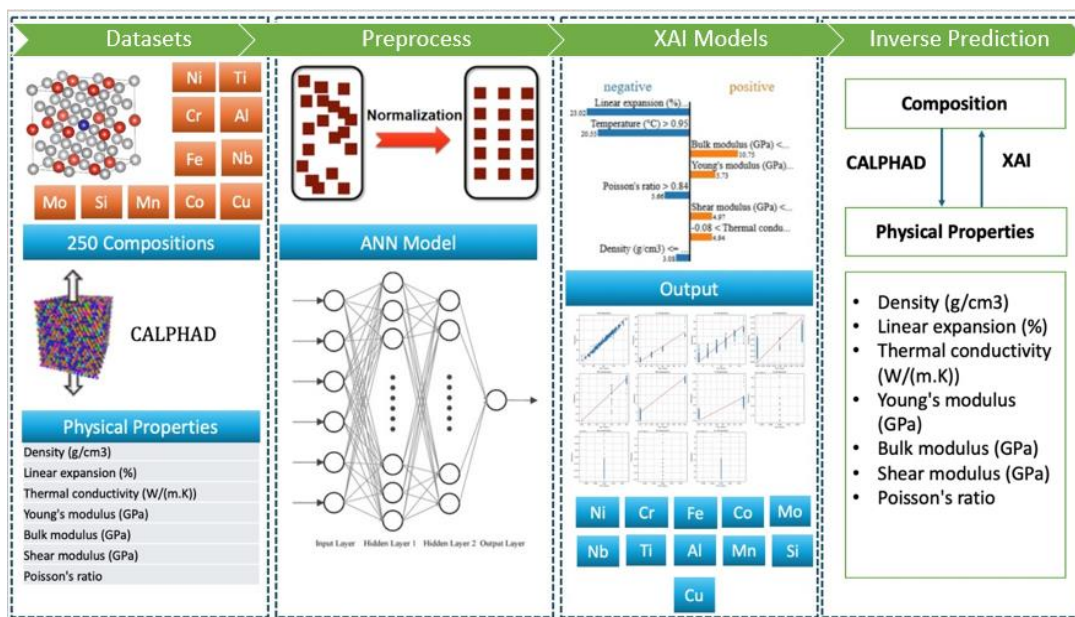

Figure 1. Proposed Model.

2.1 Dataset Generation

This study focuses on Ni-Cr-Fe (Inconel, Incoloy) alloys, which are among the most widely used superalloys in industry due to their high mechanical properties and ability to undergo precipitation hardening through solution treatment and aging. Ni-Cr-Fe (Inconel and Incoloy) alloys can be subjected to heat treatment processes, such as precipitation hardening, which helps stabilize the microstructure and maintain mechanical properties over prolonged periods at elevated temperatures. Precipitation hardening is a critical process that enhances the high-temperature strength of Inconel and Incoloy alloys [11].

The composition of JMatPro is based on the elements Ni, Cr, Fe, Co, and Mo, which constitute Ni-Cr-Fe alloys. Elements such as Nb, Ti, Al, Mn, Si, and Cu [12], which enable precipitation hardening and aging processes, are held constant at specific values across all alloys. This approach aims to discover a composition with superior mechanical properties due to precipitation hardening. The composition includes elements in the following weight percentages: Ni (50-75%), Cr (14-21%), Fe (5-15%), Co (1-2%), and Mo (2-3%), in various combinations. Additionally, the elements Nb (1 and 5%), Ti (1 and 2.5%), Al (0 and 0.5%), Mn (0.5 and 1%), Si (0.5%), and Cu (0.5%) were maintained at fixed values across all combinations. For each generated composition, Phase Fraction Diagrams and TTT diagrams were developed.

Table 1. Elemental Composition Ranges of Alloys in the Dataset (values represent wt.%).

Ni	Cr	Fe	Co	Mo	Nb	Ti	Al	Mn	Si	Cu
50-75	14-21	5-15	0-2	0-3	1, 5	1, 2.5	0, 0.5	0.5, 1	0.5	0.5

In the above table, 250 distinct compositions were generated from various combinations within the specified elemental ranges. For each composition, a total of 20 different temperature points were set in the range of 540–920 °C, with increments of 20 °C. For each temperature point, the density, thermal conductivity, linear expansion percentage, Young's modulus, bulk modulus, shear modulus, and Poisson's ratio were recorded in the dataset under the corresponding temperature entries. Consequently, physical properties corresponding to 20 temperature values were listed for each composition, resulting in a dataset comprising 5000 rows out of 250 compositions.

Table 2. The First Two Compositions (C1, C2) in the Dataset.

Composition	Alloying Elements (wt%)	Temperature (°C)	Density (g/cm3)	Linear expansion (%)	Thermal conductivity (W/(m. K))	Young's modulus (GPa)	Bulk modulus (GPa)	Shear modulus (GPa)	Poisson's ratio
C1	Ni: 67% Cr: 22%	920.0	7.78093	1.71729	26.32702	137.58134	144.72433	51.27665	0.34156
	Fe: 5%	900.0	7.79575	1.65069	25.87496	140.06745	146.50224	52.23848	0.34065
	Co: 0% Mo: 0%	880.0	7.80998	1.58694	25.45285	142.4019	148.15905	53.14259	0.33981
	Nb: 1%	⋮	⋮	⋮	⋮	⋮	⋮	⋮	⋮
	Ti: 2.5% Al: 0.5%	580.0	7.97686	0.8564	20.56181	169.22063	165.62852	63.63024	0.32972
	Mn: 1%	560.0	7.98607	0.81695	20.26687	170.75849	166.52779	64.23843	0.3291
	Si: 0.5% Cu: 0.5%	540.0	7.99514	0.77821	19.97256	172.27884	167.40553	64.84051	0.32848
C2	Ni: 66% Cr: 22%	920.0	7.78113	1.71474	26.39128	138.42486	145.55014	51.59361	0.34149
	Fe: 5%	900.0	7.79587	1.64846	25.94167	140.87727	147.30295	52.54247	0.3406
	Co: 1% Mo: 0%	880.0	7.81003	1.58504	25.52172	143.1844	148.93875	53.43608	0.33977
	Nb: 1%	⋮	⋮	⋮	⋮	⋮	⋮	⋮	⋮
	Ti: 2.5% Al: 0.5%	580.0	7.97642	0.85662	20.6351	169.93475	166.32878	63.8987	0.32972
	Mn: 1%	560.0	7.98564	0.81714	20.33941	171.47479	167.22758	64.50784	0.3291
	Si: 0.5% Cu: 0.5%	540.0	7.99472	0.77837	20.04428	172.99739	168.10489	65.11089	0.32848

As an example, the dataset created for only two alloy compositions is shown in the table above. For each composition, physical property values were recorded at 20 different temperatures ranging from 540 °C to 920 °C. In the second alloy (C2), unlike the first alloy (C1), an additional 1% Co was included. It was observed that the addition of 1% Co led to an increase in density, thermal conductivity, Young's modulus, bulk modulus, and shear modulus, while causing a decrease in linear expansion and Poisson's ratio. As demonstrated by these two examples, the physical property values for 250 different alloy combinations, modified within the ranges specified in Table 1, were added to the dataset under the corresponding temperature rows, resulting in a dataset of 5000 rows, as shown in Table 2.

Completing missing data is crucial to ensuring the integrity of the dataset. In this study, missing values were estimated using multiple linear regression based on the available data. Additionally, since the data obtained from JMatPro software were in different formats, they were converted to international SI units and standardized in terms of density (g/cm³), thermal conductivity (W/(m·K)), and expansion (%). To enable the artificial intelligence model to effectively learn the data, all physical properties were scaled between 0 and 1 using the Min-Max Normalization method and transformed into a tensor structure. Following these processes, data consistency was verified through statistical analyses by comparing with the original JMatPro values, ensuring the dataset's suitability for modeling.

2.2   Software Used for the CALPHAD Methodology

The datasets required to train the AI model were obtained using JMatPro software, which operates based on the CALPHAD methodology. In JMatPro, phase-fraction diagrams and TTT diagrams were generated by adding alloying elements to nickel at specified ratios. The diagrams created for each composition were analyzed to determine the appropriate heat treatment temperature that would yield the desired microstructure through precipitation hardening. The physical property values that the alloy would attain at this specified heat treatment temperature were then organized based on the temperature.

Each composition was simulated with appropriate heat treatment parameters to achieve the formation of the gamma, gamma prime, and gamma" phases. Phases such as delta, eta, laves, MC, M6C, and M3B2 were disregarded because they form only during long precipitation periods. Because the simulations were conducted under equilibrium conditions, the model prevented the formation of unwanted phases. The grain size of the matrix phase (gamma) was set to 100 microns. The grain sizes of the gamma prime and gamma" phases precipitating within the matrix phase were specified as 10 μm and 50 μm, respectively. For each composition, the heat treatment temperature and duration parameters were optimized to complete the precipitation of the gamma prime and gamma" phases within the matrix phase.

The JMatPro software performs Gibbs free-energy calculations, which are fundamental to the CALPHAD methodology. Gibbs free energy (G) provides information on a system's equilibrium state and phase formation.

$$G = H - TS \qquad (1)$$

where:

H: Enthalpy (total heat content),

T: Absolute temperature,

S: Entropy (measure of disorder).

Enthalpy calculations are performed using standard formation enthalpies of pure elements and alloys. The enthalpy expression used in the CALPHAD model can be expanded to include the enthalpy changes of a phase as follows:

$$H = Href + \int_{Tref}^{T} Cp \, dT \qquad (2)$$

where:

Href: Enthalpy at the reference temperature,

Cp: Heat capacity.

In the CALPHAD methodology, phase equilibria are determined by equalizing the chemical potentials of the components. The chemical potential (μi) for each component is calculated from the derivatives of the Gibbs free energy:

$$\mu i = \frac{\partial G}{\partial n i} \tag{3}$$

where *ni* represents the mole quantity of the component.

To determine phase equilibrium, the chemical potentials of each component must be equalized as follows:

$$\mu_i^\alpha = \mu_i^\beta \tag{4}$$

where α and β represent two different phases in equilibrium.

The heat capacity (*Cp*), which varies with temperature, is calculated and often expressed in polynomial form:

$$Cp = a + bT + cT^2 + dT^3 + \cdots \tag{5}$$

The coefficients (*a,b,c,d*) in this equation are determined based on experimental data or theoretical models.

JMatPro performs these calculations in the background to process the material data in its database. As a result of these processes, the phase structure of the input composition can be modeled and the thermodynamic, physical, or mechanical properties of this phase structure can be simulated with high accuracy.

In this study, JMatPro software was selected due to its superior features. One of the advantages of JMatPro over software like Thermo-Calc is its ability not only to perform thermodynamic calculations but also to predict mechanical and physical properties. JMatPro has the capacity to calculate properties of metal alloys such as phase transformations, elastic and plastic deformation characteristics, fatigue, and creep. In this regard, it offers a broader scope compared to Thermo-Calc, which mainly focuses on phase diagrams and equilibria [13].

Another significant advantage of JMatPro over Thermo-Calc is its ability to integrate engineering approaches into alloy development processes. This provides researchers with greater flexibility and accuracy in the design and optimization of new materials. Thus, it offers a solution that focuses not only on phase diagrams but also on the detailed prediction of mechanical properties [14].

With these superior features, JMatPro can create a model that approximates the mechanical properties of the generated composition. Consequently, in this project, the mechanical property data required to train artificial intelligence can be modeled in the software without the need for time-consuming experimental studies.

2.3 Development of the Artificial Intelligence Model

The artificial intelligence (AI) model developed in this study combines Explainable Artificial Intelligence (XAI) techniques with Artificial Neural Networks (ANNs) to facilitate the inverse prediction of physical properties in Ni-Cr-Fe-based superalloys. This model aims to overcome the limitations of traditional CALPHAD approaches by predicting alloy compositions with specified mechanical and thermal properties, thus optimizing the design process and reducing the reliance on trial and error.

2.3.1 Data Preparation and Model Architecture

A comprehensive training dataset was created, including data on density, thermal conductivity, linear expansion, Young's modulus, bulk modulus, shear modulus, and Poisson's ratio. The data were divided into training (80%) and validation/testing (20%) sets using a method widely applied to ensure robust model performance.[15].

ANNs were chosen for their capacity to model nonlinear, high-dimensional relationships, which are typical in complex alloy systems. Recent studies have demonstrated that ANNs can handle multivariable datasets and accurately model the dependencies in alloy properties when integrated with domain knowledge from materials science [16]. The model architecture includes several hidden layers optimized for neuron count and activation functions, enabling efficient learning of complex patterns while maintaining computational efficiency [17].

Ensuring the completeness of missing data is crucial for maintaining the integrity of the dataset. In this study, missing values were estimated using multiple linear regression based on

the available data. Additionally, since the data obtained from JMatPro software were provided in various formats, they were converted into international SI units and standardized into metrics such as density (g/cm³), thermal conductivity (W/(m·K)), and expansion (%). To allow the artificial intelligence model to effectively learn the data, all physical properties were scaled between 0 and 1 using the Min-Max Normalization method and then transformed into a tensor structure. Following these processes, data consistency was verified through statistical analyses by comparing the results with the original JMatPro values, ensuring the dataset's readiness for modeling.

2.3.2 Training and Optimization

The model was trained over 500 epochs, utilizing Mean Absolute Error (MAE) as the loss metric to minimize the error between the predicted and actual values. Figure 3(a) shows the rapid decrease in both training and validation losses in the initial epochs, followed by stabilization at epoch 100, indicating the model's learning plateau. This training approach, which is supported by backpropagation and gradient descent, is common in materials informatics applications where data complexity is high [18].

To enhance the model's generalizability and prevent overfitting, regularization techniques, such as dropout layers, were implemented. Studies have shown that such regularization methods are effective for improving the robustness of models in predictive material science, allowing models to generalize beyond the training dataset [19].

2.3.3 Explainable AI for Feature Analysis

To enhance interpretability, SHAP (SHapley Additive exPlanations) values were applied to assess feature importance in the ANN model. The XAI analysis revealed that linear expansion, temperature, and Poisson's ratio were the most influential predictors of alloy properties (Figure 2). The application of XAI techniques is essential in materials science, where understanding the relationship between compositional variables and property outcomes is critical for effective alloy design [20].

2.3.4 Model Performance Evaluation

The ANN model achieved an accuracy rate of 98.03%, closely approximating the JMatPro-generated values for key physical properties (Table 3). The high accuracy of the proposed model aligns with recent advancements in ANN-based alloy prediction models, which

demonstrate that machine learning models can provide reliable predictions that are comparable to traditional simulation methods [21]. This model's successful application validates the potential of integrating CALPHAD and AI approaches, paving the way for future AI-enhanced alloy design frameworks.

This work contributes to a growing body of research that uses machine learning to facilitate alloy design and property prediction, demonstrating the potential of AI to advance materials science beyond traditional methods [22] [23] [24].

3   RESULTS AND DISCUSSION

The artificial intelligence (AI) model developed for predicting the physical properties of Ni-Cr-Fe-based superalloys has demonstrated notable accuracy, achieving an overall prediction accuracy rate of 98.03%. This success is indicative of the model's potential to effectively aid alloy design by accurately predicting compositions that meet the target property requirements. The accuracy analysis shown in Table 3 reveals that the AI model's predictions closely align with the values obtained from JMatPro simulations, with minor deviations observed across different properties. This alignment underscores the reliability of the AI approach as a complementary tool to CALPHAD-based methodologies.

Table 3. Comparison of Desired Physical Properties with Values Obtained by Modeling the AI-Suggested Compositions in JMatPro and Their Accuracy Rates.

Composition Suggested by AI	Physical Properties at 920°C	Suggested Values of Composition to be Offered by AI	Values Obtained by Modeling the Composition Suggested by the AI Model in JMatPro	Accuracy (%)
Ni: 69.23 % Cr: 15.05 % Fe: 9.45 % Co: 1.33 % Mo: 0.54 % Nb: 0.39 % Ti: 1.46 % Al: 0.51 % Mn: 1.02 % Si: 0.51 % Cu: 0.51 %	Density (g/cm3)	7.9	7.91415	99.820886
	Linear expansion (%)	1.59	1.65911	95.653459
	Thermal conductivity (W/(m. K)	27.7	28.34599	97.667906
	Young's modulus (GPa)	146	142.92744	97.895506
	Bulk modulus (GPa)	157.5	153.9451	97.742920
	Shear modulus (GPa)	54.4	53.1225	97.651654
	Poisson's ratio	0.346	0.34526	99.786127
			Overall Accuracy (%):	**98.03**

In Table 3, the comparison between the target values of the suggested composition and the actual values obtained via JMatPro modeling illustrates a high level of congruency across key properties such as density, linear expansion, thermal conductivity, Young's modulus, bulk modulus, shear modulus, and Poisson's ratio. Each of these properties was predicted with an accuracy rate close to or exceeding 97%, with density and Poisson's ratio achieving exceptionally high accuracy rates of 99.82% and 99.79%, respectively. This high accuracy rate reflects the AI model's proficiency in capturing the intricate relationships between elemental composition and physical properties at elevated temperatures, specifically at 920 °C.

To gain a deeper understanding of how different input features influence AI model predictions, we employed Explainable Artificial Intelligence (XAI) techniques. The XAI analysis, as illustrated in the feature importance graph, indicates that linear expansion, temperature, and Poisson's ratio are among the most influential factors affecting the AI model's predictions. The SHAP (SHapley Additive exPlanations) values highlight that a higher linear expansion and temperature exert a positive impact on the prediction output, whereas parameters like density, bulk modulus, Young's modulus, and shear modulus have a more negative influence.
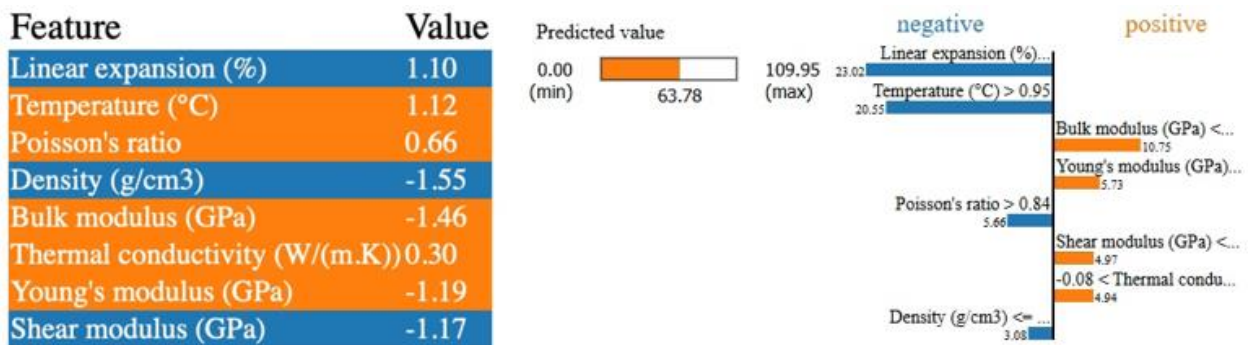

Figure 2. Effect of Physical Properties on Prediction.

Figure 2 presents the feature importance and impact analysis performed using SHAP (SHapley Additive exPlanations) values with Explainable Artificial Intelligence (XAI) techniques. Each feature's contribution to the model's prediction is shown on a scale ranging from negative to positive impact, with orange bars representing positive contributions and blue bars indicating negative contributions. The model's predicted value (63.78) falls within the possible range of 0–109.95.

Features such as linear expansion (%) and temperature (°C) exhibited positive impacts on the prediction outcome, with linear expansion contributing the highest positive value (23.20)

and temperature following closely (20.55). This suggests that an increase in these parameters tends to raise the predicted value, likely due to their direct relationship with the thermal behavior of alloys.

In contrast, features such as density (g/cm³), bulk modulus (GPa), shear modulus (GPa), Young's modulus (GPa), and thermal conductivity (W/(m. K)) exert negative influences. Among these, the bulk modulus has the most substantial negative effect (-10.75), followed by Young's modulus (-5.73). This negative impact indicates that higher values for these properties might correlate with a reduction in the model's target prediction, likely reflecting the mechanical rigidity of the alloy.

Poisson's ratio, while having a minor impact compared to the other features, shows a slightly negative influence, which is consistent with the mechanical and deformation behavior characteristics at various temperatures.

This insight into feature importance aligns with the underlying physics of Ni-Cr-Fe superalloys, where thermal expansion and mechanical stability at high temperatures are crucial factors in determining material performance. The model's ability to prioritize features that are inherently critical to alloy behavior demonstrates the model's interpretability and the potential of XAI to enhance trust in AI-driven alloy design.

The model's learning process over 500 epochs is visualized in the training and validation loss graphs, which show a significant decline in both training and validation losses as epochs progress. By the end of training, the losses converged, indicating that the model effectively minimized the errors without overfitting to the training data. Additionally, the Mean Absolute Error (MAE) graph reinforces this finding, as both the training and validation MAE values stabilize around low values, confirming the model's generalizability.
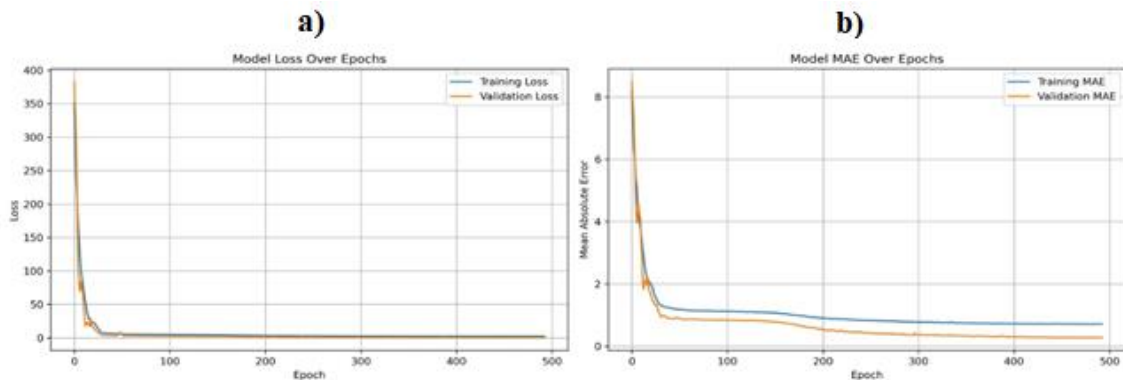

Figure 3. Model Loss and Mean Error Graphs Over Epochs: (a) Model Loss Graph, (b) Model Mean Absolute Error (MAE) Graph.

Figure 3(a) shows the loss of the machine learning model over 500 training epochs. The loss values for both the training and validation data decreased rapidly in the initial epochs and stabilized around epoch 100. This indicates that model performance has reached a plateau. Figure 3(b) shows the Mean Absolute Error (MAE) of the model for training and validation data over 500 epochs. The MAE values initially decreased rapidly and then stabilized, similar to the loss curve. The consistency between the training and validation MAEs indicates that the model achieves good generalizability without overfitting.
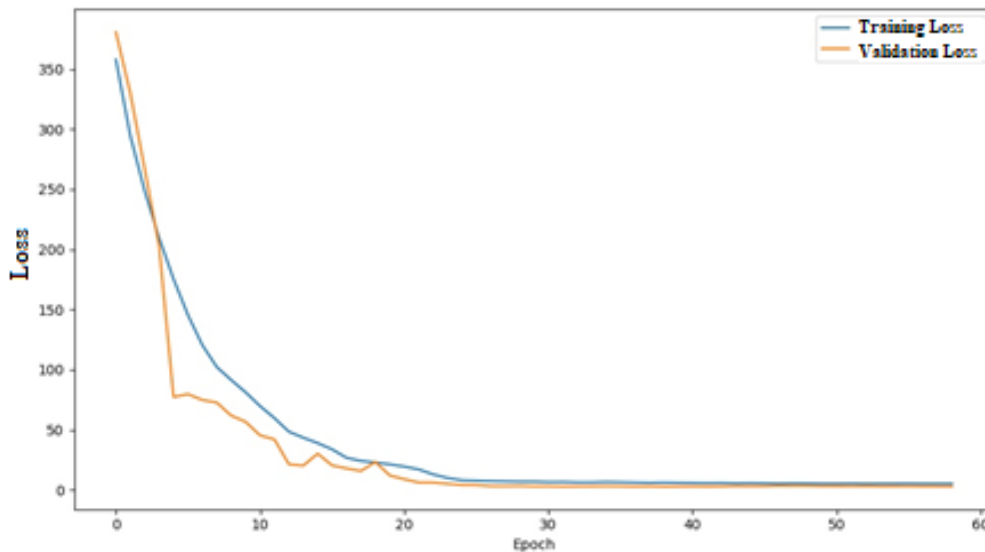

Figure 4. Training and Validation Loss Graph.

The rapid decrease in training and validation losses in early epochs (Figure 4) demonstrates the model's ability to quickly learn the relationships within the dataset. As training continued, the loss reduction became more gradual, suggesting that the model was fine-tuning its predictions. The convergence of training and validation losses at lower error rates reflects a balanced model that can maintain accuracy across unseen data.

Table 4 summarizes the error metrics used to evaluate the performance of the artificial neural network model. MSE (0.2245) and MAE (0.2742) numerically demonstrate the proximity of the model's predicted physical properties to the actual values. MSE is particularly important for understanding the magnitude of prediction errors, as it penalizes larger errors more heavily. The R^2 score (0.5504) indicates that the model can explain approximately 55% of the total variance. These results suggest that the model demonstrates reasonable performance but requires additional optimizations for improved outcomes.

Table 4. Evaluation of Model Performance Based on Error Metrics.

Error Metrics	Value	Description
Mean Squared Error (MSE)	0.2245	The mean of the squared differences between predicted and actual values. Larger errors are penalized more heavily.
Mean Absolute Error (MAE)	0.2742	The average of the absolute differences between predicted and actual values.
Coefficient of Determination (R^2)	0.5504	A measure that indicates the proportion of the variance in the dependent variable explained by the model (%55 in this case).

The AI model's predictions were validated against the JMatPro outputs, which follow the CALPHAD methodology. As shown in the graphical and tabular data, the AI model consistently approximated JMatPro's physical property values with high accuracy. This demonstrates the potential of AI for efficient and reliable inverse alloy design. Unlike CALPHAD, which requires intensive calculations and adjustments, the AI model rapidly processes large datasets to deliver accurate predictions, offering a significant time-saving advantage.

Moreover, the use of Explainable AI provides a transparent view into the AI model's decision-making process, which is traditionally seen as a "black box" in neural network-based models. This transparency adds value by allowing researchers to understand the weight and impact of each feature, thus enhancing the model's applicability in real-world alloy design.

The results obtained from this study reveal that integrating CALPHAD-generated data with artificial intelligence, specifically with the support of XAI, offers a transformative approach to alloy design. This AI-driven framework not only enhances prediction accuracy and provides insights into the compositional dependencies of physical properties at high temperatures. This capability is especially valuable in designing high-performance superalloys for demanding applications such as aerospace and power generation, where precise control over properties like thermal conductivity, modulus, and expansion is crucial.

In conclusion, the AI model, validated using CALPHAD data, was found to be effective in predicting the physical properties of Ni-Cr-Fe-based superalloys with high accuracy. The use of XAI further strengthens the model's reliability and interpretability, making it a valuable tool for future alloy development. This study demonstrates a significant advancement in materials science, paving the way for more efficient and accurate alloy design processes driven by AI, which can be extended to other alloy systems in future research.

4   CONCLUSION AND SUGGESTIONS

In this study, a novel approach integrating the CALPHAD methodology with artificial intelligence, specifically Explainable Artificial Intelligence (XAI) and Artificial Neural Networks (ANN), was demonstrated to predict alloy compositions with desired physical properties for Ni-Cr-Fe-based superalloys. The AI model achieved a high prediction accuracy of 98.03%, thereby validating the efficacy of this inverse prediction approach in alloy design. By using JMatPro software to generate comprehensive datasets and applying XAI to interpret model outputs, this study provides a reliable and transparent method for optimizing superalloy compositions.

The results indicate that this AI-driven framework can significantly reduce the trial-and-error processes traditionally required for alloy design, thus saving time and resources. The integration of XAI also enhances the model's interpretability, allowing researchers to understand the influence of individual elements on alloy properties. This interpretability is crucial for practical applications because it helps identify optimal compositional ranges that meet specific mechanical and thermal requirements.

Suggestions for Future Work:

Expansion to Other Alloy Systems: Future research could extend this methodology to other alloy systems, such as Ti-based or Al-based alloys, to explore its generalizability and applicability across diverse materials.

Incorporation of Additional Properties: Including additional properties, such as creep resistance, fatigue strength, and corrosion resistance, could improve the model's relevance for specific industrial applications, particularly in aerospace and energy sectors where such properties are critical.

Real-World Validation: The experimental validation of AI-predicted compositions in real-world manufacturing and testing environments will provide further insights into the model's accuracy and practical feasibility.

Optimization of Model Architecture: Exploring different neural network architectures or hybrid machine learning models, such as ensemble learning techniques, may yield further improvements in prediction accuracy and computational efficiency.

Development of an Automated Alloy Design Platform: Combining CALPHAD and AI methods into an automated platform for alloy design could streamline the process for materials scientists, enabling rapid prototyping of alloys tailored to meet specific engineering requirements.

In conclusion, the integration of CALPHAD-generated data with advanced AI techniques represents a transformative approach to alloy design. This study demonstrates the potential of AI to complement traditional materials science methods, paving the way for efficient, data-driven alloy development. Future advancements in this field are expected to enhance the capabilities of AI in alloy design, enabling more sophisticated and customizable solutions in materials engineering.

Conflict of Interest Statement

There is no conflict of interest between the authors.

Statement of Research and Publication Ethics

The study is complied with research and publication ethics.

Artificial Intelligence (AI) Contribution Statement

This manuscript was entirely written, edited, analyzed, and prepared without the assistance of any artificial intelligence (AI) tools. All content, including text, data analysis, and figures, was solely generated by the authors.

Contributions of the Authors

Yusuf Uzunoğlu: Conceptualization, methodology, data curation, resources, and writing-original draft. Yusuf Alaca: Supervision, validation, visualization, formal analysis and writing-review & editing.

REFERENCES

[1]   N. Saunders and A. P. Miodownik, *CALPHAD (Calculation of Phase Diagrams): A Comprehensive Guide*. Pergamon Press, 1998.

[2]   H. L. Lukas, S. G. Fries, and B. Sundman, *Computational Thermodynamics: The Calphad Method*. Cambridge University Press, 2007.

[3]   Y. Du, S. L. Chen, and B. Huang, "An Overview of CALPHAD Applications in Superalloy Design," *J. Alloys Compd.*, vol. 456, no. 1–2, pp. 18–29, 2008.

[4]   P. Raccuglia and others, "Machine-learning-assisted materials discovery using failed experiments," *Nature*, vol. 533, no. 7601, pp. 73–77, 2016.

[5]   T. Xie and J. C. Grossman, "Crystal Graph Convolutional Neural Networks for an Accurate and Interpretable Prediction of Material Properties," *Phys. Rev. Lett.*, vol. 120, no. 14, p. 145301, 2018.

[6]   K. T. Butler and others, "Machine learning for molecular and materials science," *Nature*, vol. 559, no. 7715, pp. 547–555, 2018.

[7]   L. Ward et al., "A general-purpose machine learning framework for predicting properties of inorganic materials," *npj Comput. Mater.*, vol. 2, no. 1, pp. 1–7, 2016.

[8]   D. Jha and others, "ElemNet: Deep Learning the Chemistry of Materials from Only Elemental Composition," *Sci. Rep.*, vol. 8, no. 1, pp. 1–13, 2018.

[9]   Y. Zhang and others, "Deep learning-based discovery of rare materials," *Nature*, vol. 569, no. 7754, pp. 368–373, 2019.

[10]   B. L. DeCost and others, "Scientific AI in materials science: A Pathway to Discovery and Insight," *MRS Bull.*, vol. 45, no. 8, pp. 614–623, 2020.

[11]   X. Zhang, "Heat treatment effects on Inconel alloys.," *J. Mater. Eng.*, 2019.

[12]   A. S. M. I. H. Committee and A. S. for M. H. T. Division, *Heat treating*, vol. 4. ASM international, 1991.

[13]   P. Palumbo, G., & Ferro, "Comparison of CALPHAD-based tools for materials science applications.," *J. Phase Equilibria Diffus.*, no. 34(5), pp. 398–405, 2013.

[14]   A. P. Zhao, J. C., Miodownik, "CALPHAD and its applications to materials science," *Prog. Mater. Sci.*, no. 51(3), pp. 241–312, 2006.

[15]   C. Chen, J. Zhao, and L. Li, "Machine Learning for Alloy Design: An Overview of Recent Advances," *Mater. Today*, vol. 48, pp. 15–27, 2021.

[16]   K. Tran et al., "Active Learning Across Intermetallics to Guide Alloy Design," *Nat. Commun.*, vol. 9, p. 4074, 2018.

[17]   A. Agrawal and A. Choudhary, "Deep Learning Applications and Challenges in Big Data Analytics for Manufacturing," *Manuf. Lett.*, vol. 15, pp. 12–19, 2019.

[18]   L. Ward and C. Wolverton, "A Machine Learning Approach for Predicting and Understanding the Properties of Multiprincipal Element Alloys," *npj Comput. Mater.*, vol. 4, p. 36, 2018.

[19]   J. Schmidt and others, "Recent Advances and Applications of Machine Learning in Solid-State Materials Science," *npj Comput. Mater.*, vol. 5, p. 83, 2019.

[20]   A. Karpatne and others, "Regularization Techniques for Neural Networks: An Overview and Applicability in Materials Science," *J. Appl. Phys.*, vol. 128, no. 14, p. 141501, 2020.

[21]   J. Ling, M. Hutchinson, and C. Wolverton, "Machine Learning for Multi-Property Predictions in Computational Materials," *Comput. Mater. Sci.*, vol. 138, pp. 140–152, 2017.

[22]   Y. Zuo and others, "Accelerated Discovery of Metallic Glasses Using Machine Learning," *Mater. Horizons*, vol. 6, no. 2, pp. 252–261, 2019.

[23]   Y. Xu, J. Luo, and W. Chen, "Artificial Neural Networks in Alloy Design: Development and Challenges," *Adv. Eng. Mater.*, vol. 22, no. 4, p. 1901206, 2020.

[24]   K. Kaufmann and K. S. Vecchio, "Artificial Intelligence in Materials Science: A New Frontier," *Mater. Sci. Eng. R Reports*, vol. 144, p. 100595, 2020.